

More Than A Star: How The Sun Impacts The Heliosphere

Kamen A. Kozarev*

*Smithsonian Astrophysical Observatory
60 Garden St.
Cambridge, MA02138
E-mail: kozarev@cfa.harvard.edu*

The past decade has seen dramatic improvements in observations of the Sun and the domain influenced by its electromagnetic and plasma emission - the heliosphere. This has brought about significant advances in our understanding of how the solar corona is heated, how the solar wind is accelerated, and how solar eruptions affect the energetic particle populations in the heliosphere, on time scales from minutes to years. We overview some of the latest advances, focusing on short-term solar activity. In addition, we provide some observational and modeling insight into how eruptive reorganizations of magnetic fields and plasma, known as flares and coronal mass ejections, can create populations of very energetic ionized particles, which pose radiation risks for astronauts and satellites.

POS (BASH 2013) 011

*Frank N. Bash Symposium 2013: New Horizons in Astronomy (BASH 2013)
October 6-8, 2013
Austin, Texas*

*Speaker.

1. Introduction

The Sun, our closest star, is our best laboratory for understanding the physics of cosmic plasmas. But it is also far less peaceful than it seems from the comfort of our sheltered vantage point, the Earth. Violent and explosive reorganizations of magnetic fields in the atmosphere of the Sun cause strong bursts of emission throughout the light spectrum, known as flares. They are often accompanied by gigantic clouds of hot ion and electron plasma, called coronal mass ejections (CMEs), ejected from its surface, which travel through and affect most of the heliosphere. Finally, these explosions have been known to create and release significant fluxes of extremely high-energy charged particles, known as solar energetic particles (SEPs), which travel along interplanetary magnetic fields. Most of these particles are protons. SEPs pose a serious threat to human endeavors in space, as they can cause irreparable radiation damage to living tissues outside Earth's atmosphere, as well as damage to satellite electronics.

The discipline heliophysics studies all phenomena that occur on the Sun as well as in interplanetary space and the vicinity of planetary environments. It is experiencing an unprecedented growth, driven throughout the last two decades by the exponential growth in computing power available to solve complex problems over multiple scales and dimensions, as well as the slew of space missions that have been devoted to studying the heliosphere.

In this paper, we review some of the important recent advances in heliophysics in the past several years, focusing on solar eruptions and their effects. We also present some original work on the properties of coronal shock waves formed during solar eruptions and the processes that influence how they may produce large fluxes of SEPs.

2. Solar Activity

The main evidence of solar activity is the presence of sunspots (in white light), or more recently, the abundance of active regions in extreme ultraviolet (EUV) and X-ray observations. Even as the Sun is very stable in its white light emission, its high energy emissions vary greatly over any given cycle. The reorganization of magnetic fields seems to be an important source of energy for heating the solar corona and the solar wind. Such active region (AR) field reorganization on very short time scales is also responsible for solar eruptions - some of the most energetic impulsive events in the solar system. Figure 1 shows the manifestation of the 11-year solar activity cycle in EUV light in single representative images from every year of solar cycle 23. The increased magnetic field reorganization in active regions on the surface of the Sun causes coronal plasma to heat up and emit in EUV. Most of the emission comes from the very dynamic ARs.

We can also gain an understanding of the mid- to long-term manifestation of solar activity by studying interplanetary parameters of the solar plasma. In situ observations of the solar wind, such as the out of the ecliptic plane measurements by the Ulysses spacecraft shown in the left part of Fig. 2 have revealed that the solar wind magnetic field is organized and its speed depends on the amount of activity, as well as on its source latitude. In the first polar orbit of Ulysses (left panel), it measured fast wind near the poles where coronal holes abounded during the solar minimum period, and slow wind at low latitudes, where there was increased magnetic activity. The magnetic field was mostly of outward polarity above the equator, and inward below it. During its second orbit,

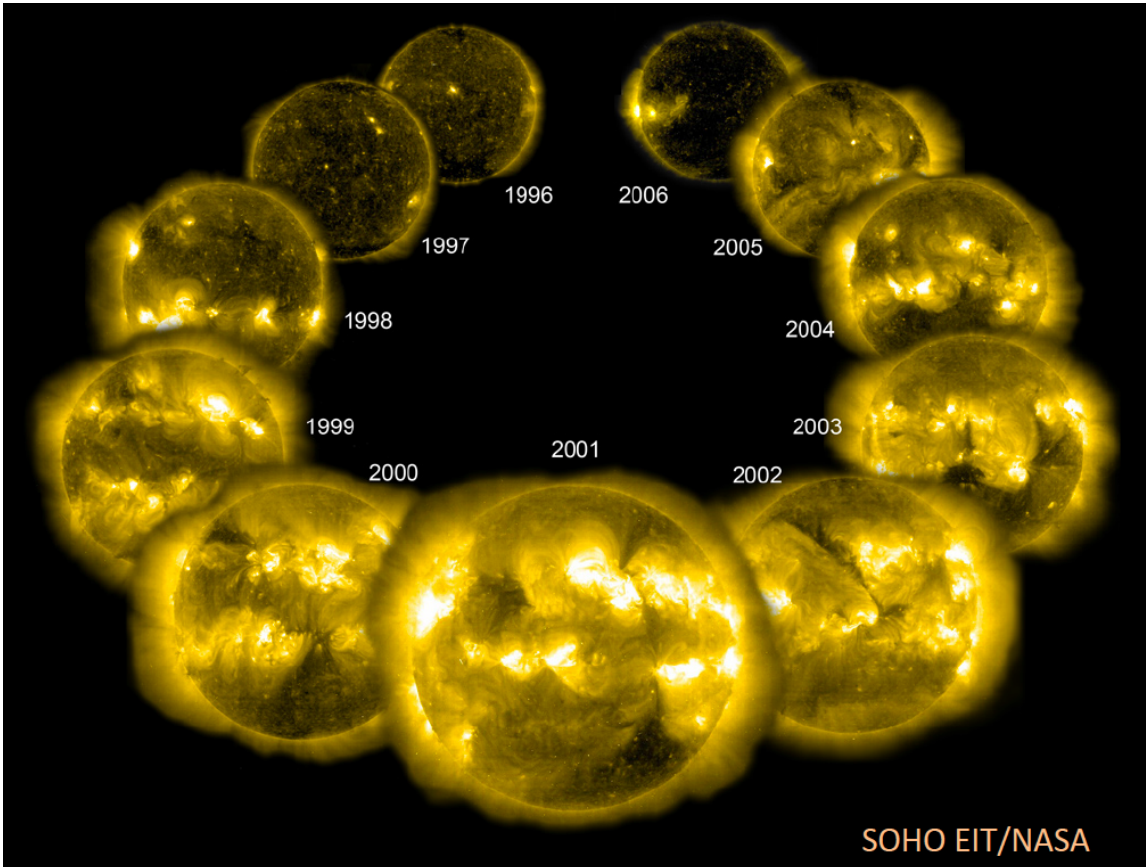


Figure 1: Solar EUV activity over a solar cycle, as seen by the Extreme Ultraviolet Imaging Telescope on board the SOHO space observatory. The increase in emission accompanies the increased magnetic activity on the surface of the Sun.

in the right panel of the left part of the figure, this well-defined behavior was gone - there was no strong dependence of latitude for the solar wind speed, as active regions spanned most of the solar surface, and large-scale magnetic field reversals were the norm. In the lower left panels, the sunspot number is plotted over time, showing the onset of the cycle maximum.

In the right part of Fig. 2, a similar period of the last solar cycle is shown, for which several other observed parameters are plotted. The top panel shows again sunspot numbers, followed by the interplanetary coronal mass ejection frequency/per month, the number of interplanetary shocks detected near 1 AU, the SEP fluxes, and the galactic cosmic ray fluxes. These are further measures of how the Sun influences the heliosphere over its cycle. The increase of sunspot numbers correlates with the observed interplanetary shocks, CME frequency, and SEP frequency, while the galactic cosmic ray fluxes are reduced significantly during the maximum, due to their deflection by the more complicated and stronger interplanetary magnetic fields.

3. Heliospheric Energetic Particle Populations

The interaction of the active Sun with the heliosphere produces different populations of energetic particles. Figure 3 shows the fluence spectrum of oxygen as measured by the ACE spacecraft

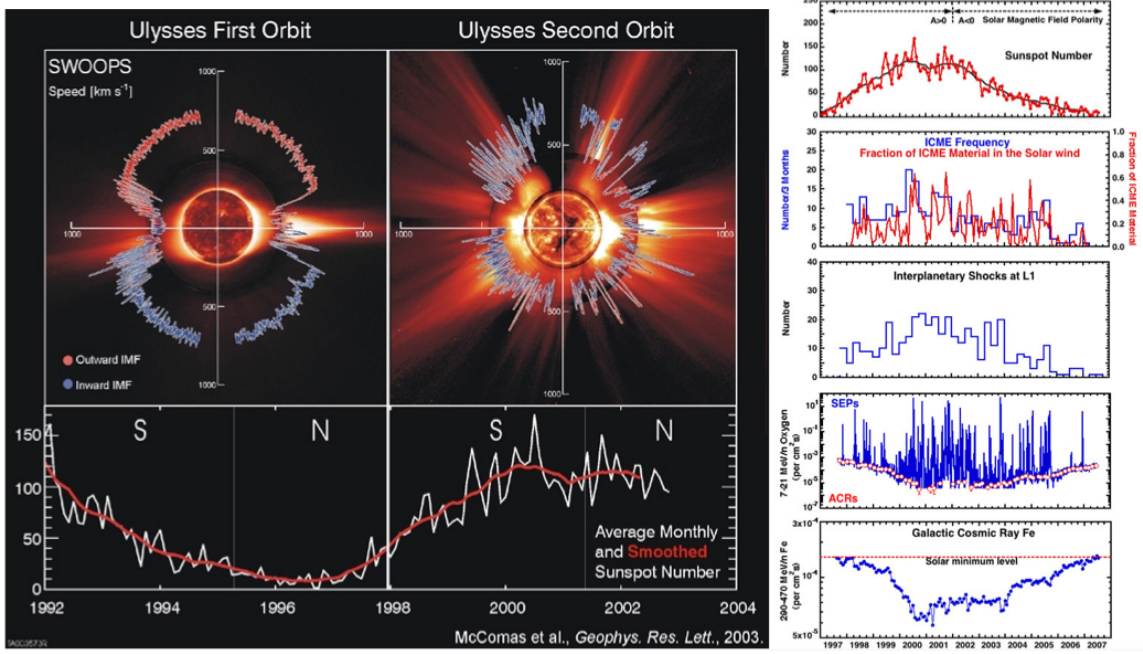
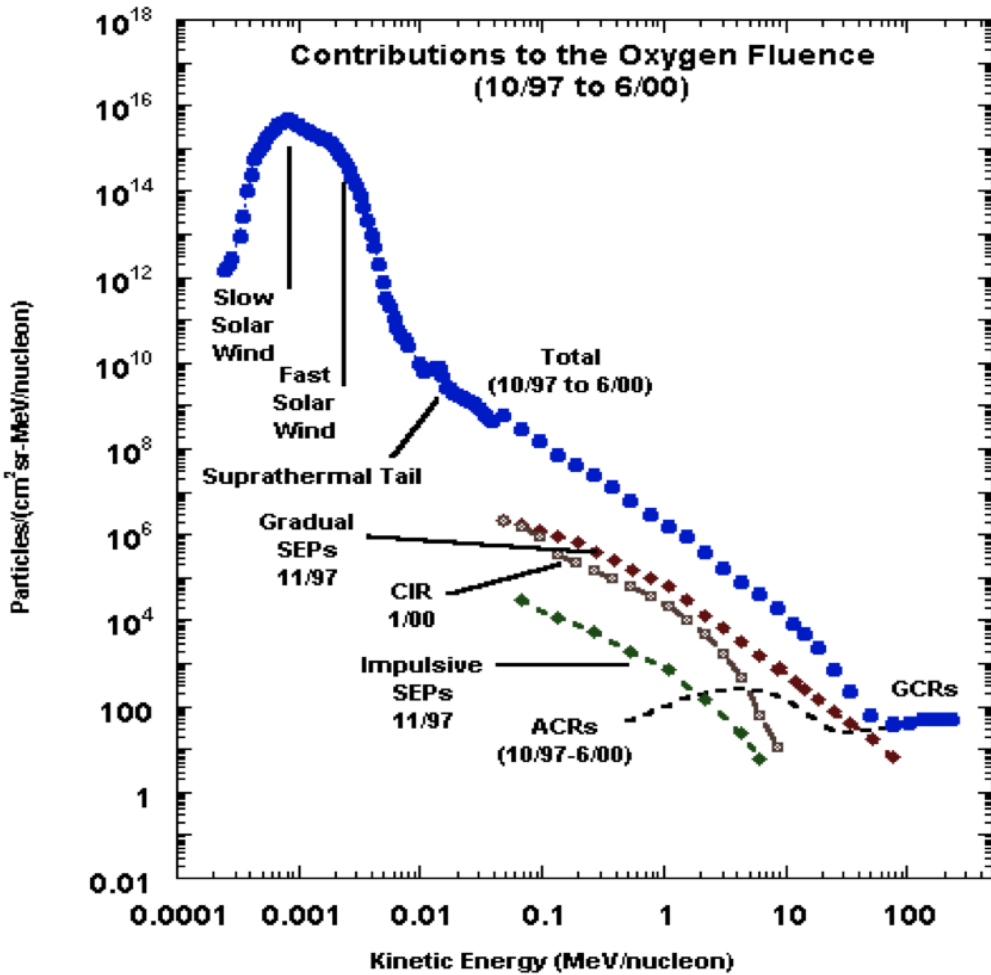


Figure 2: (Left) Solar wind speed as a function of heliospheric latitude during solar minimum (left panels) and maximum (right panels), observed in situ by the Ulysses spacecraft during two polar passages in solar cycle 23. Figure from [19]. (Right) A summary of the variability of various interplanetary observables over solar cycle 23 by the ACE spacecraft at the L1 point. Figure from <http://www.srl.caltech.edu/ACE/ACENews/ACENews109.html>.

from [20]. This plot illustrates the general differentiation between the different particle populations in the heliosphere. At the low-energy end of the spectrum is the thermal plasma distribution of the bimodal solar wind, consisting of a slow and a fast component. It usually peaks around 1 keV/nucleon. Suprathermal particles are a population with energies above the solar wind distribution thermal peak. They are not important for space weather predictions, but are often invoked as a possible quiet time source distribution, from which SEPs are accelerated during flares and in CME-driven shocks. They extend in energy between roughly 0.01-1 MeV. Energetic particles of solar origin ('impulsive' and 'gradual' SEPs) make up the fluxes between 1-100 MeV in energy. Charged particles accelerated by co-rotating interaction regions (CIRs) also contribute to the fluences in that energy range. Finally, Galactic cosmic rays (GCR) are a distinct population of charged energetic particles with origins outside of the solar system that show up as increases in the fluxes above several hundred MeV. These particles represent a radiation background of steady fluxes that are modulated by solar magnetic fields. For this reason, GCR fluxes increase further out in the heliosphere. Anomalous cosmic rays (ACR) are another population of energetic particles, thought to be accelerated by the heliospheric termination shock, that are not very common near Earth.

Historically, SEP events have been classified into two types of events - 'gradual' and 'impulsive', corresponding to the impulsive or gradual X-ray flares that accompany them. Initially, it was thought that SEPs were related exclusively to solar flares, which were thought to accelerate particles in both types of events, depending on whether the flare was gradual or impulsive. Later, it was realized that they also occur in relation to interplanetary shocks. [9] showed that there is a



POS (BASH 2013) 011

Figure 3: A representative spectrum of long-term Oxygen fluences observed by the ACE spacecraft, showing different particle types. Figure from [20]

strong correlation between the temporal occurrence of strong SEP events and CMEs, and that the speeds and angular extent of the CMEs observed in white light coronagraph images are correlated with the strength of the in situ SEP fluxes. In the 1970s a new kind of event was discovered, which exhibit very high ratios of ${}^3\text{He}/{}^4\text{He}$, as well as high charge states in the minor ions [15]. These are small events, unrelated to interplanetary shocks. This reinforced the ‘impulsive’ and ‘gradual’ event classification.

However, in situ observations in the 1990s and 2000s revealed a lot of hybrid events, with signatures of both flare and shock acceleration [27, 3]. Some of the events had time intensity profiles consistent with shock acceleration, but with compositions seen in impulsive flare-associated events. Some very large events were related to impulsive soft X-ray flares with no shocks observed. This

forced a review of the simple picture of two types of events. The SEP paradigm shifted toward a more comprehensive view in which part of the acceleration would be provided by flares in the corona, and the rest by interplanetary shocks.

Starting in the early 2000s, shocks were reported in coronagraph observations [30, 34], and also indirectly as coronal particle accelerators [8]. MHD modeling studies showed that shocks could indeed exist in the corona [18]. SEPs may also be created in the corona due to transient, fast, compressive flows.

4. Coronal Mass Ejections and Flares

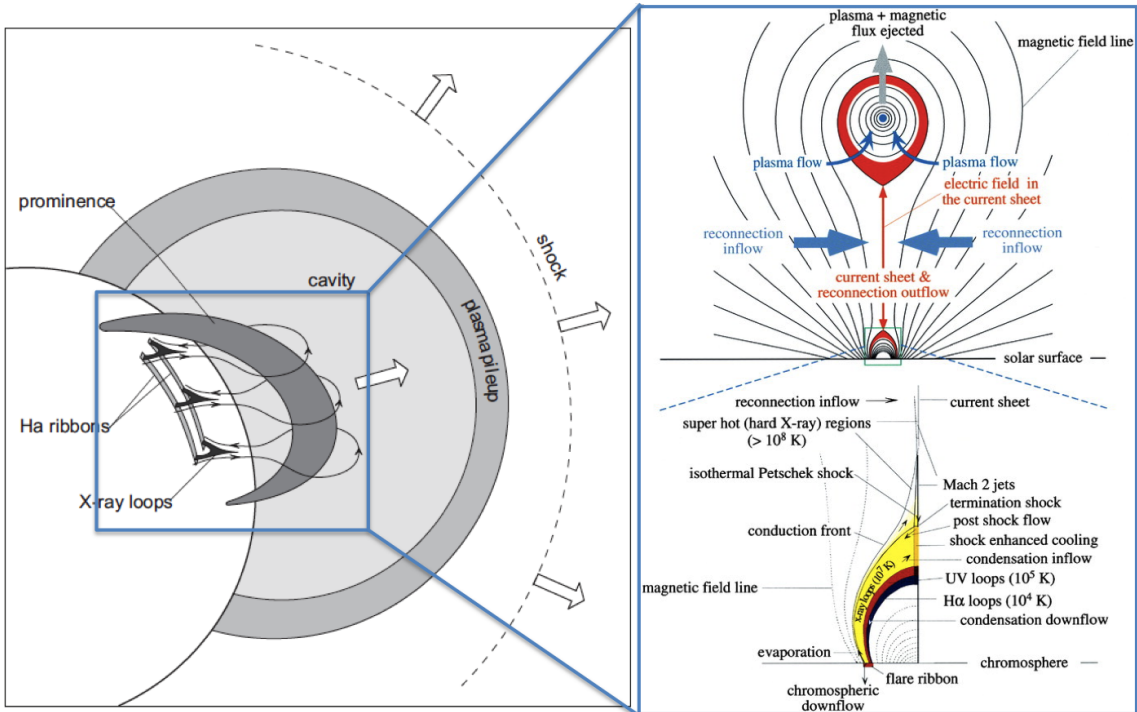


Figure 4: The current view of solar eruptions. On the left is the global structure of a CME (figure taken from [6]), while on the right is a detailed look at the vertical structure and conditions of an idealized eruption (figure taken from [14]).

The main manifestations of solar activity on time scales of minutes to days are solar eruptions. These usually consist of Coronal Mass Ejections (CMEs) and flares. CME refers to the ejection of plasma clouds with embedded magnetic fields, while flares are taken to mean all the electromagnetic emission produced in these impulsive events. Flares and CMEs are usually complementary. Solar eruptions occur throughout the solar cycle, but are much more common near the peak of solar activity. They release vast amounts of energy - up to 10^{33} ergs per event. Many of them drive shock waves that accelerate charged particles to solar energetic particle (SEP) energies. The acceleration and heliospheric propagation of large SEP fluxes during solar flares and CMEs are of considerable interest to heliophysics and interplanetary physics not only because they probe solar system magnetic fields, but also because they may pose significant radiation hazard to astronauts and spacecraft electronics beyond low-earth orbit.

Figure 4 synthesizes the prevalent view on how CMEs are formed and the phenomena that occur during their initial phases. On the left is a global cartoon of the first stage of a CME. The driver of the eruption is a magnetic flux rope (a collection of closely-spaced field lines), formed through continuous slow reconnection between AR loops, which are brought together through bringing their photospheric footpoints, as well as shearing and rotating them. Thus, the flux rope has a typical helical arcade-like magnetic structure. This prominence (or filament) rests on the tension produced by the underlying magnetic field loops, and is trapped by overlying magnetic loops. At a certain point, the pressure balance between the flux rope and the strapping fields above it is destroyed by a kink or torus MHD instability, at which point the flux rope begins to detach from the Sun. This reduces the magnetic pressure behind it, causing the strapping loops around it to come together and reconnect behind it, further speeding up the flux rope. Reconnection heats the plasma on these loops, leading to emission in H α and X-rays at the base of the eruption. This emission constitutes a flare. Note that, according to some authors, reconnection and flare emission begin first, driving the destabilization of the flux rope. Once the prominence has gained super-Alfvenic speed, it drives a fast shock in front of it. If the CME over-expands significantly in the lateral direction, plasma in front of it may not be able to escape, forming a pile-up region between the flux rope and the shock front.

On the right of Fig. 4 is a closer view at the beginning of the eruption and the associated phenomena, when the CME is viewed edge-on. The red, teardrop-shaped feature near the top is the flux rope, which contains field lines wrapped around the core inside. It is surrounded by stretched coronal field lines. The ejecta cause the overlying loops to reconnect below it, forming a long, thin current sheet. Reconnection heats the local plasma by converting magnetic into kinetic and thermal energy in the newly formed currents and electric fields. Some of the plasma is ejected upwards to the core of the CME, while the rest is directed back to the surface of the Sun. The small-scale loops that form near the surface as a result of the reconnection are known as post-flare loop arcades. The inset on the lower right of the figure describes what occurs in that region. A significant amount of rapidly heated plasma becomes trapped on these loops, emitting in EUV and X-rays. Much of the plasma accelerated by the relaxation of the loops collides with the chromospheric material near its footpoints, creating the so-called ‘ribbons’. There may be termination shocks present near the edges of the reconnection regions.

The final result is hot coronal plasma ejected in the interplanetary CME, as well as constrained to the low-coronal flare post-flare loops. Some of the coronal plasma is further heated and accelerated in the reconnection region behind the CME, in the direct electric fields as well as by the ‘slingshot’ effect of relaxing magnetic field loops. In terms of energetic particles, this is considered the flare population, although the mechanism discussed here does not allow much of these particles to actually leave the solar atmosphere, since they’re mostly confined to closed loops near the surface. In contrast, the coronal and interplanetary plasma ahead of the flux rope are accelerated by the shock wave and in pile-up regions, and are able to escape upstream of the CME along heliospheric magnetic field lines.

5. Properties of Coronal Waves and Shocks

Fast global disturbances in the solar atmosphere were reported first by Moreton [21] in H α

observations. The disturbances (called Moreton waves) had transverse velocities between 500 and 2500 km/s and appeared to be activated by flares, but were localized in the chromosphere. Similar global disturbances were observed much higher, in the corona, at EUV wavelengths when the Extreme-ultraviolet Imaging Telescope (EIT) on board the SOlar and Heliospheric Observatory (SOHO) spacecraft first observed the Sun in 1997 [32]. These 'EIT waves' (also known as coronal bright fronts - CBFs, or merely as EUV waves) appeared as broad, diffusive, arc-shaped regions of brighter EUV emission. These observations revived the topic of shocks and waves in the corona, and a variety of observational and theoretical studies followed. Further observations of EIT waves showed that they have speeds between 100 and 700 km/s [35], may displace coronal magnetic structures, and have a Gaussian-like front cross section [37].

Two conflicting sets of theories emerged to explain the EUV wave phenomenon: one suggested that these were MHD waves, dispersive or soliton [36]; the other interpreted it as the reorganization of the magnetic field during CME eruptions and reconnection [1]. The ambiguity was further fuelled by the low spatial and temporal cadence of the EIT instrument. More recent multi-point and high cadence observations from the STEREO spacecraft have provided strong evidence that EIT waves should really be treated as truly three-dimensional phenomena, and not just surface disturbances. [33] were able to observe a wave event which started on disk and continued off the limb. In addition, they showed that the EUV wave front in that event coincided with the CME leading edge position in the white light coronagraph.

A host of observations in the last several years have revealed properties of coronal waves, as well as how they relate to other coronal phenomena. Waves are often accompanied by type II metric radio bursts, which are attributed to coronal shocks [25]. They have been observed to reflect and refract at coronal hole boundaries [16], and in general their propagation is influenced by the local magnetic topology [22]. They affect all layers of the solar atmosphere [31], and can spread along vast areas of the surface. The waves can be observed above the coronal limb as well, and often have the shape of a dome enveloping the erupting flux rope. Overall, they seem to appear if the speed of the CME expansion overtakes the local fast-mode speed [24]. The waves are often initially driven by the CME, but later decouple and propagate freely.

6. Coronal Shocks As Particle Accelerators

Coronal shock signatures are often associated with SEP events. However, to date little detailed work has been done on how, where, and when energetic particles get accelerated in shocks traveling through the corona. In depth simulations of particle acceleration have been performed for idealized magnetic fields to test theories of diffusive acceleration [7]. Recent numerical magnetohydrodynamic (MHD) simulations of realistic CMEs show that the diffusive shock acceleration process can accelerate SEPs to more than 1 GeV [10]. Most global models focus on interplanetary space beyond ~ 10 solar radii, neglecting the important and dynamic environment of the corona between 1.2 and 10 solar radii. Thus, realistic global simulations of the coronal magnetic fields and plasma environment, of traveling shocks, and of energetic particles, constrained by modern observations, are needed to tackle the question of shock acceleration in the corona adequately and in detail.

Coronal shock signatures are often associated with SEP events. This is based on observational evidence of shock-related signatures in the corona such as large-scale coronal (EIT) waves, spectral

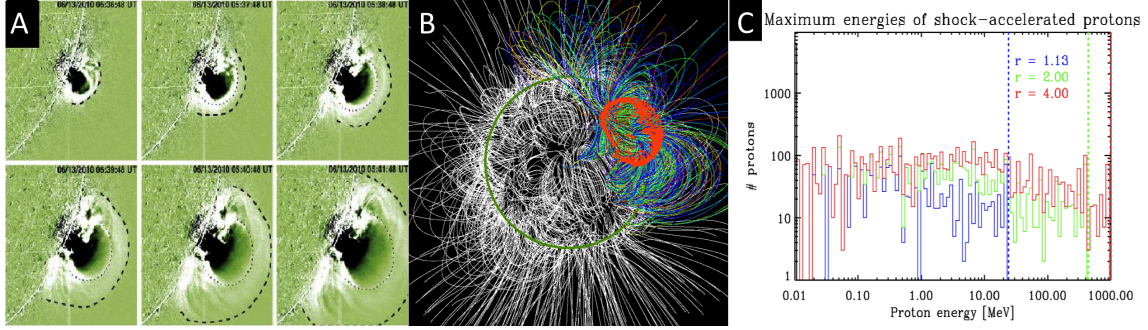


Figure 5: A: EUV observations of the June 13, 2010 western CME and shock event. The dashed lines show the shock front, and the CME bubble is denoted with a dotted line. B: The shock crossing points projected onto the shock surface, color coded with the field-to-shock angles. C: Histograms of final proton energies for three shock speed and strength combinations. The initial energy distribution is in black, and the vertical dashed lines show the highest energies reached for each setup.

line shifts, white-light coronagraph images, and metric radio bursts. Remote observations have suggested [5], and confirmed [33, 17] that shocks may form as low as $0.2 R_S$ from the surface of the Sun, and certainly in the middle corona [34, 23]. UV spectroscopic and imaging observations have captured the properties of several coronal shocks [26, 2] in the low and middle corona, and revealed moderate shock strength and plasma heating in the low corona. Unfortunately, those measurements lacked the ability to follow the CME and shock evolution throughout the corona due to their low temporal (SOHO/EIT, SOHO/LASCO) or spatial resolution (SOHO/UVCS)

Recent studies have used EUV and metric radio observations to show the intimate connection between EUV waves and CME-driven shocks [4]. In recent work, we analyzed two coronal shock events using EUV observations of coronal bright fronts from the Atmospheric Imaging Assembly (AIA) instrument on the Solar Dynamics Observatory (SDO), as well as radio and in situ observations [13]. Figure 5 shows the EUV observations of the June 13, 2010 coronal wave (panel A). We showed that the EUV fronts were consistent with MHD shocks. We also showed that the magnetic field topology in which the shock propagates is crucial for determining the acceleration location and subsequent direction of release and propagation of the accelerated particles. We further applied a simple diffusive shock acceleration model applicable to the propagation of an idealized spherical shock through a coronal potential field source surface model [28, PFSS], and estimated the energization of protons with initial energies of 0.01 MeV [12]. Figure 5, panel B shows the PFSS coronal field with the spherical shock model; panel C shows histograms of the final proton energies for three different shocks. We found that fast, quasi-perpendicular shocks can accelerate protons in the corona to more than 100 MeV. What is more, the shock speed, strength, and orientation to the magnetic fields control the amount of energization. Work continues on characterizing high-cadence EUV observations of the solar corona, in order to characterize multiple off-limb eruptive events in terms of their shock dynamics and proton acceleration efficiencies, and develop a framework for estimating coronal SEP source distributions.

To study in more detail how CME-driven shocks accelerate charged particles to SEP energies very close to the Sun, we have used realistic global simulations. We have developed and used a

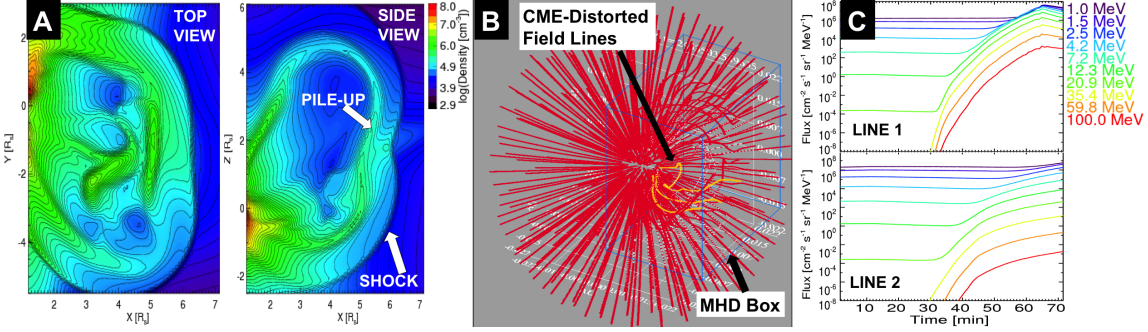


Figure 6: A. Top (left) and Side (right) views of plasma density at a late stage of the CME simulation. The shock and pile-up region are denoted. B. The EPREM grid at one time step of the simulation. Some CME-distorted field lines are shown in yellow inside the box where MHD parameters from the CME simulation are used. C. Simulated SEP Fluxes at $8 R_S$ on two field lines - Line 1 near the region of greatest CME expansion, Line 2 near a region of slowest expansion.

global numerical model for transport and acceleration of charged particle distributions [29]. In recent work [11], we coupled this model to realistic CME MHD simulation results. Using a detailed coronal and CME model has allowed us to take into account the realistic, time-dependent properties of the CME and shock, magnetic field orientations, and local solar wind parameters in the particle acceleration and transport simulation. We have shown (Figure 6, panel C) that the acceleration efficiency varies along different field lines, and may depend on CME overexpansion into low pressure coronal regions resulting in the formation of plasma pile-ups.

7. Summary

Solar eruptions are one of the main phenomena that affect space weather in the heliosphere. They can influence the interplanetary and planetary environments over vast longitudinal and radial ranges by injecting fast solar wind plasma, increased magnetic flux, and highly energetic ions and electrons. In this paper, we have attempted to give a brief overview of the current understanding of solar cycle variability, and in particular of the initial stages of CMEs - the most energetic solar system plasma phenomena. We have sought to relate CMEs to the production of high energy particles early in eruptions.

Coronal shock signatures are often associated with SEP events. This is based on observational evidence of shock-related signatures in the corona such as large-scale coronal (EIT) waves, spectral line shifts, white-light coronagraph images, and metric radio bursts. The observations imply that significant particle acceleration may occur in shocks immediately after the eruption onset. In addition, the existence of shock-acceleration this low in the corona reinforces a paradigm shift - from the idea that SEP events may be either impulsive (due to flare acceleration) or gradual (due to interplanetary shock acceleration) - to one admitting hybrid events with both flare- and shock-accelerated particles. In fact, coronal shocks may account for most of the impulsive phase SEP fluxes. This has been supported by recent original work presented here, which suggests that 1) shock waves are ubiquitous in the initial phase of solar eruptions, and 2) they may easily accelerate protons to hundreds of MeV energies in the low and middle corona.

Acknowledgments

The author would like to thank the Frank Bash Symposium committee for the kind invitation.

References

- [1] Attrill, G. D. R., Harra, L. K., van Driel-Gesztelyi, L., Démoulin, P. 2007, *Astrophys. J. Lett.*, 656, L101
- [2] Bemporad, A. & Mancuso, S. 2010, *Astrophys. J.*, 720, 130
- [3] Cane, H. V., von Rosenvinge, T. T., Cohen, C. M. S., & Mewaldt, R. A., 2003, *Geophys. Res. Lett.*, 30, 120000
- [4] Carley, E. P., Long, D. M., Byrne, J. P., Zucca, P., Shaun Bloomfield, D., McCauley, J., & Gallagher, P. T. 2013, *Nature Physics*
- [5] Cliver, E. W., Kahler, S. W., & Reames, D. V. 2004, *Astrophys. J.*, 605, 902
- [6] Forbes, T. G. 2000, *J. Geophys. Res.*, 105, 23153
- [7] Giacalone, J. 2005, *Astrophys. J. Lett.*, 628, L37
- [8] Haggerty, D. K. & Roelof, E. C. 2002, *Astrophys. J.*, 579, 841
- [9] Kahler, S. W., Sheeley, Jr., N. R., Howard, R. A., Michels, D. J., Koomen, M. J., McGuire, R. E., von Rosenvinge, T. T., & Reames, D. V. 1984, *J. Geophys. Res.*, 89, 9683
- [10] Kóta, J., Manchester, W. B., Jokipii, J. R., de Zeeuw, D. L., & Gombosi, T. I. 2005, in American Institute of Physics Conference Series, Vol. 781, The Physics of Collisionless Shocks: 4th Annual IGPP International Astrophysics Conference, ed. G. Li, G. P. Zank, & C. T. Russell, 201–206
- [11] Kozarev, K. A., Evans, R. M., Schwadron, N. A., Dayeh, M. A., Opher, M., Korreck, K. E., & van der Holst, B. 2013, *Astrophys. J.*, 778, 43
- [12] Kozarev, K. A., Korreck, K. E., Lobzin, V. V., & Schwadron, N. A. 2012, in Proceedings of the Fifth Hinode Conference, Astronomical Society of the Pacific Conference Series
- [13] Kozarev, K. A., Korreck, K. E., Lobzin, V. V., Weber, M. A., & Schwadron, N. A. 2011, *Astrophys. J. Lett.*, 733, L25
- [14] Lin, J., Raymond, J. C., & van Ballegooijen, A. A. 2004, *Astrophys. J.*, 602, 422
- [15] Lin, R. P. 1974, *Space Sci. Rev.*, 16, 189
- [16] Long, D. M., Gallagher, P. T., McAteer, R. T. J., & Bloomfield, D. S. 2008, *Astrophys. J. Lett.*, 680, L81
- [17] Ma, S., Raymond, J. C., Golub, L., Lin, J., Chen, H., Grigis, P., Testa, P., & Long, D. 2011, *Astrophys. J.*, 738, 160
- [18] Manchester, IV, W. B., Vourlidas, A., Tóth, G., Lugaz, N., Roussev, I. I., Sokolov, I. V., Gombosi, T. I., De Zeeuw, D. L., & Opher, M. 2008, *Astrophys. J.*, 684, 1448
- [19] McComas, D. J., Elliott, H. A., Schwadron, N. A., Gosling, J. T., Skoug, R. M., & Goldstein, B. E. 2003, *Geophys. Res. Lett.*, 30, 100000

- [20] Mewaldt, R. A., Mason, G. M., Gloeckler, G., Christian, E. R., Cohen, C. M. S., Cummings, A. C., Dwyer, J. R., Gold, R. E., Krimigis, S. M., Leske, R. A., Mazur, J. E., Stone, E. C., von Rosenvinge, T. T., Wiedenbeck, M. E., & Zurbuchen, T. H. 2001, in International Cosmic Ray Conference, Vol. 10, International Cosmic Ray Conference, 3984
- [21] Moreton, G. E. 1960, *Astron. J.*, 65, 494
- [22] Olmedo, O., Vourlidas, A., Zhang, J., & Cheng, X. 2012, *Astrophys. J.*, 756, 143
- [23] Ontiveros, V. & Vourlidas, A. 2009, *Astrophys. J.*, 693, 267
- [24] Patsourakos, S. & Vourlidas, A. 2012, *Sol. Phys.*, 281, 187
- [25] Pick, M. 2008, in COSPAR Meeting, Vol. 37, 37th COSPAR Scientific Assembly, 2431
- [26] Raymond, J. C., Thompson, B. J., St. Cyr, O. C., Gopalswamy, N., Kahler, S., Kaiser, M., Lara, A., Ciaravella, A., Romoli, M., & O'Neal, R. 2000, *Geophys. Res. Lett.*, 27, 1439
- [27] Reames, D. V. 1999, *Space Sci. Rev.*, 90, 413
- [28] Schrijver, C. J. & De Rosa, M. L. 2003, *Sol. Phys.*, 212, 165
- [29] Schwadron, N. A., Townsend, L., Kozarev, K., Dayeh, M. A., Cucinotta, F., Desai, M., Golightly, M., Hassler, D., Hatcher, R., Kim, M., Posner, A., PourArsalan, M., Spence, H. E., & Squier, R. K. 2010, *Space Weather*, 8, 0
- [30] Sheeley, N. R., Hakala, W. N., & Wang, Y.-M. 2000, *J. Geophys. Res.*, 105, 5081
- [31] Shen, Y. & Liu, Y. 2012, *Astrophys. J.*, 754, 7
- [32] Thompson, B. J., Plunkett, S. P., Gurman, J. B., Newmark, J. S., St. Cyr, O. C., & Michels, D. J. 1998, *Geophys. Res. Lett.*, 25, 2465
- [33] Veronig, A. M., Muhr, N., Kienreich, I. W., Temmer, M., & Vršnak, B. 2010, *Astrophys. J. Lett.*, 716, L57
- [34] Vourlidas, A., Wu, S. T., Wang, A. H., Subramanian, P., & Howard, R. A. 2003, *Astrophys. J.*, 598, 1392
- [35] Wang, Y.-M. 2000, *Astrophys. J. Lett.*, 543, L89
- [36] Wills-Davey, M. J., DeForest, C. E., & Stenflo, J. O. 2007, *Astrophys. J.*, 664, 556
- [37] Wills-Davey, M. J. & Thompson, B. J. 1999, *Sol. Phys.*, 190, 467